Research Article

Guixia Wang* and Junhong Su

Study on the impulse mechanism of optical films formed by laser plasma shock waves

https://doi.org/10.1515/phys-2022-0237
received October 19, 2022; accepted February 23, 2023

Abstract: In a high-power laser system, when the surface pressure of the optical film caused by laser plasma shock wave is greater than the adhesion per unit area of the film layer, the film will produce mechanical damage, and in serious cases, the whole system may not work. Therefore, studying the formation mechanism of optical film surface pressure and impulse caused by laser plasma shock wave is the key to ensure the normal operation of the high-power laser system. In this article, by studying the relaxation process of laser plasma shock wave on the surface pressure of optical film, and using the time accumulation effect of various pressures on the surface of the optical film, the calculation model of impulse on the optical film's surface formed by laser plasma shock waves was established, and the variation rules of the impulse I_{st} and impulse coefficient j on the unit area of single-layer Al_2O_3 and HfO_2 optical films with different parameters were obtained. When the incident laser wavelength λ was 1,064 nm, the energy E was , the pulse width t_p was 10 ns, the focal length of the focusing lens f was 350 mm, the distance between the film surface and the focal plane of the focusing lens z_0 was 5 mm, and the film radius R was 5 mm, the calculation and simulation results show that the impulse I_{st} of the two films was 10^{-4} N s order of magnitude, the impulse coefficient j of the two films was 10^{-5} N s/J, the Al_2O_3 film with small atomic number will obtain larger I_{st} and j, I_{st} and j of the two films increase with the increase of E and f, and I_{st} and j of the two films decrease with the increase of z_0 and t_p. In the total impulse transfer time (t_0), I_{st} and j both increase with the increase of R.

Keywords: film plasma, shock wave, impulse, impulse coupling coefficient

1 Introduction

Generally speaking, in the initial stage of laser–optical film interaction, heat action heats the film and makes it locally heated, which leads to the increase of free electrons or gasification of the film. When the concentration of free electrons and ions reaches a certain amount, optical breakdown (indicating that the optical film has undergone irreversible changes, that is, failure) occurs, and then, plasma is formed [1–5]. The absorption of subsequent laser energy by plasma causes its own temperature to rise sharply, and its volume expands outward after reaching a high temperature and overheating state, that is, the plasma shock wave is formed [6–8], and the initial propagation speed of plasma shock wave reaches the order of magnitude of 10^4 m/s. As a result, mechanical action is generated on the optical film surface, and the film surface obtains impulse during the interaction between the plasma shock wave and the optical film surface. The magnitude of the impulse is not only related to the action laser parameters, such as energy, pulse width, and spot size, but also closely related to the properties of the action film materials and the action environment. The calculation of the impulse obtained by the film with different incident laser parameters can not only understand the mechanism of the plasma shock wave on the film impulse transfer, and the relationship between the efficiency and the laser parameters, but also have a certain reference value for the technology of using laser as the propulsion power source.

At present, much research has been done on the impact of laser-induced plasma shock wave on the target surface. In 1966, Gregy and Thomas of the University of California studied the impulse of a ruby giant pulse laser on a surface in a vacuum, and experimentally measured the impulse obtained by targets of different materials [9]. In 1972, Pirri *et al.* used high-power CO_2 to act on carbon

* **Corresponding author: Guixia Wang,** Department of Photoelectric Engineering, Xi'an Technological University, 2 Xuefu Zhonglu, Wei yang District, Xi'an, Shaanxi, 710021, China, e-mail: noragirl6@126.com
Junhong Su: Department of Photoelectric Engineering, Xi'an Technological University, 2 Xuefu Zhonglu, Wei yang District, Xi'an, Shaanxi, 710021, China

Open Access. © 2023 the author(s), published by De Gruyter. This work is licensed under the Creative Commons Attribution 4.0 International License.

targets and tungsten targets, measured the impulse obtained by the targets, and tried to explain these impulses from the theory of explosive waves [10]. In 1976, Hettche *et al.* measured the impulse of pulsed CO_2 laser on aluminum target by the target pendulum technology, and measured the change process of target surface pressure during pulse by the optical interference technology, and found out the dependence of target surface pressure and applied laser power density [11]. In 1980, Duzy *et al.* studied the impulse coupling coefficient of 353 nm XeF laser irradiation on aluminum target at 0.1 Torr ambient pressure [12]. Bass *et al.* measured the impulse coupling coefficient of the long-pulse Nd glass laser on the aluminum target and found that the impulse coupling coefficient is related to the convergence/divergence characteristics of the laser when penetrating the material, and it is inversely proportional to the migration quality of the target. At the same time, the authors also gave the relationship between the impulse coupling coefficient and the laser power density, and the relationship between the impulse coupling coefficient and the energy density [13]. Fu and Wang from the Institute of Mechanics, Chinese Academy of Sciences used the impulse matrix method to measure the impulse caused by TEA CO_2-intense laser acting on the target, and also carried out the pressure measurement of shock wave induced by intense pulsed laser in the air [14–16]. In 2020, Liang *et al.* summarized the measurement methods of impulse coupling coefficient, mainly including impact pendulum method, laser interference method, laser-combined impact pendulum method, horizontal guide rail measurement method, pressure sensor method, *etc.*, and introduced the main numerical analysis methods and influencing factors of impulse coupling coefficient [17]. In 2020, Yu *et al.* studied the impulse generated by ablating aluminum targets using the micro-impulse measurement method with a torsion pendulum, and the plasma plume characteristics were researched using fast photography and optical emission spectroscopy [18]. In 2022, Xu *et al.* used impulse measurement, spectral diagnostics, temporal evolution images, and target ablation to investigate the dynamic behaviors and parameters of Nd:YAG nanosecond laser-induced aluminum plasma at different pressures and laser fluence [19]. These works provide a lot of experimental data and results for the study of laser–target interaction, and lay a solid experimental foundation for the theoretical model research. However, these works mainly focus on the experimental measurement of target impulse, while the research on the formation mechanism of target surface impulse is relatively few; the optical film is different from the general target, and its interaction with laser is more complex. Therefore, in this article, the single-layer Al_2O_3 and HfO_2 films are taken as examples (the single-layer Al_2O_3 and HfO_2 film substrates are both quartz substrates, and their optical thickness is $\lambda/4$ nm, in which the wavelength is λ = 1,064 nm); this article intends to analyze the generation of optical film surface impulse from the aspects of surface pressure generation and plasma formation during the interaction between laser and optical film surface, establish the calculation model of optical film surface impulse, and calculate the optical film surface impulse under different parameter conditions. The influence of various parameters on the surface impulse of optical films is obtained, which reveals the formation mechanism of laser plasma shock wave on the surface impulse of optical films.

2 Theoretical calculation model of optical film surface impulse

The impulse on the optical film surface formed by the laser plasma shock wave is the time cumulative effect of the shock wave on various pressures. According to the generation and formation mechanism of various pressures in the process of laser and optical film, the formation of impulse and its calculation model can be discussed. The impulse calculation of optical film surface has the following two cases.

2.1 When the breakdown threshold of the optical film surface is not reached

When the applied laser power density does not reach the breakdown threshold of the optical film surface, the impulse on the unit area of the optical film surface formed by the laser has only two parts: one is the impulse caused by the light pressure itself, whereas the second is the recoil impulse caused by the material sprayed on the optical film surface.

1) The optical pressure

When high-power pulsed laser light acts on the surface of the optical film, considering the optical pressure p_p, there are [20]

$$p_p = P/c, \tag{1}$$

where P is the incident laser power density and c is the speed of light. If the incident laser is a Q-switched laser, the pulse width is generally of the order of ns. If $P = 10^9$ W/cm^2, then $p_p = 3.33 \times 10^4$ N/m^2 = 33 kPa.

When the laser-focusing spot diameter is 0.8 mm, the pulse width is 10 ns, the energy is 0.1 J, and the wavelength is 1, 064 nm, the impulse caused on the optical film is the product of light pressure, the laser-focusing spot, and time, namely [20]:

$$P_{\mathrm{p}} \times \pi \times (0.8 \div 2 \times 10^{-3}) \times 10 \times 10^{-9} = 1.67 \times 10^{-10}\ \mathrm{N\ s}. \quad (2)$$

2) Pressure produced by the ejected material

When the high-power laser is applied to the surface of the optical film, the surface temperature of the film is heated by the laser beam, and its surface temperature rises rapidly. When the vaporization temperature is reached, a Knudsen layer with high-temperature gas and liquid phases will be formed on the surface of the film, and the thickness of the layer is about 10^{-7} m. Because the layer continues to absorb laser pulse energy, on the one hand, the temperature continues to rise, and, on the other hand, the substances in the layer quickly leave the film surface in the form of vapor, that is, spray substances are formed [20]. The velocity of ejected material particles is Maxwell distribution, which can be characterized by a characteristic velocity. The average velocity of vapor particles can characterize the macroscopic behavior of the ejected material, namely [20]:

$$\overline{v} = \sqrt{\frac{8R_{\mathrm{g}}T}{\pi M_{\mathrm{mol}}}}, \quad (3)$$

where R_{g} is the molar gas constant, $R_{\mathrm{g}} = 8.31432\ \mathrm{J/(mol\ K)}$, T is the temperature of steam, and M_{mol} is the molar mass of ejected material.

Suppose that when a pulsed laser with energy E acts on the optical film surface, the ejected mass of the film material is Δm, and its mass mobility v_{m} is defined as the mass of ejected material that can be taken away by the laser beam with unit energy. In fact, when the ejected material is ejected outward, according to the impulse theorem, the optical film surface also has a recoil impulse, so the recoil impulse I_{I} per unit area is [20]:

$$I_{\mathrm{I}} = \Delta m \overline{v} = v_{\mathrm{m}} E \sqrt{\frac{8R_{\mathrm{g}}T}{\pi M_{\mathrm{mol}}}}. \quad (4)$$

If the applied laser is a Q-switched laser, the mass mobility v_{m} is about 1–10 μg/J (μg/J indicates how much microgram (μg) mass can be migrated by 1 J laser energy on the surface of the film), taking the single-layer HfO_2 film as an example, if $E = 0.1$ J, $t_p = 10$ ns, $M_{\mathrm{mol}} = 210.49$ g/mol, $T = 3{,}031$ K, then I_{I} is about 7.56×10^{-8} N s.

Obviously, when the applied laser power density does not reach the breakdown threshold of the optical film surface, the impulse caused by the light pressure is about two orders of magnitude smaller than the recoil caused by the ejected material. At this time, the impulse of the laser on the unit area of the film surface mainly depends on the recoil caused by the ejected material.

2.2 When the breakdown threshold of the optical film surface is reached

When the applied laser power density is greater than the breakdown threshold of the film surface, the impulse formed by the plasma shock wave on the unit area of the film surface consists of three parts: one is the impulse caused by the light pressure itself; second is the recoil impulse caused by ejected materials; the third is the impulse generated by the expansion and diffusion of laser plasma shock wave.

It can be seen from the previous analysis that the impulse caused by light pressure is about 1.67×10^{-10} N s, and this impulse is far less than the impulse caused by ejected material and plasma shock wave, so it can be ignored. The mass of splashed material is also very small, and the impulse I_{I} introduced is about 7.56×10^{-8} N s. This order of magnitude impulse is not dominant in the interaction between laser and optical film surface, and can also be ignored. Therefore, when the applied laser power density is greater than the breakdown threshold of the film surface, the impulse on the optical film surface is mainly generated by the expansion and diffusion of the plasma shock wave, which will be mainly discussed below.

When the applied laser power density is greater than the breakdown threshold of the optical film surface, the optical film surface is broken down and a plasma shock wave is generated. The plasma shock wave generates great pressure on the film, making the optical film obtain impulse. If the time distribution of the pressure generated after the plasma shock wave acts on the film surface is $p_{\mathrm{s}}(t)$, and I_{s} is used to represent the impulse obtained on the unit area of the film, then:

$$I_{\mathrm{s}} = \int_0^{t_0} p_{\mathrm{s}}(t)\mathrm{d}t, \quad (5)$$

where t_0 is the total action time of laser plasma shock wave. Therefore, the film impulse mainly depends on

the pressure $p_s(t)$ of the expansion and diffusion of the plasma shock wave on the film surface, which is calculated below.

2.2.1 Pressure produced by the expansion and diffusion of plasma shock wave

During the pulse laser irradiation, the plasma on the thin film surface ignites, expands rapidly outward, and rapidly develops into laser supported detonation wave (LSDW). This absorption wave continues to absorb the residual pulsed laser energy and expands away from the film surface, and produces a pressure p_{s10} on the film surface. However, the pulse width of the laser pulse is limited, and the disturbance behind the LSDW wave cannot catch up with LSDW during the pulse laser action. LSDW preferentially absorbs the laser pulse energy and propagates at the supersonic speed, so the intensity of LSDW would not weaken. LSDW mainly expands in the reverse direction of laser, which can be approximately regarded as one-dimensional flow field. The motion of LSDW would change after the end of the laser pulse. First, the intensity of LSDW would decrease with the propagation process. Second, the propagation of LSDW has no laser energy absorption in the opposite direction of the laser, so there is no priority. The lateral sparsity becomes important, and the motion of LSDW should be regarded as a two-dimensional flow field.

If the laser pulse width is t_p and the characteristic time of LSDW two-dimensional motion is defined as t_{2D}, which is equal to the time required for LSDW wavefront to expand to the distance of focused spot diameter (D_s), then [20]:

$$D_s = \frac{2\lambda f}{\pi d}\left[1 + \left(\frac{\pi z_0 d^2}{\lambda f^2}\right)^2\right]^{\frac{1}{2}}. \tag{6}$$

$$v_L = 0.958\rho_0^{-\frac{1}{3}}P^{\frac{1}{3}}. \tag{7}$$

$$t_{2D} = D_s/v_L. \tag{8}$$

In Eq. (6), λ is the wavelength of the incident laser beam, d is the diameter of the incident laser beam, f is the focal length of the focusing lens, and z_0 is the distance between the surface of the film and the focal plane of the focusing lens. In Eq. (7), ρ_0 is the air density, $\rho_0 = 1.295\,\mathrm{kg/m^3}$, and P is the power density of the incident laser; in Eq. (8), v_L is the propagation speed of the LSDW.

Use P_0 to represent the initial power density of the incident laser. When the incident laser energy is E, there are:

$$P_0 = \frac{4E}{\pi {D_s}^2 t_p}. \tag{9}$$

P_1 and P_2 are used to represent the radiation loss in the plasma region and the radiation loss caused by the reverse bremsstrahlung absorption of the laser passing through LSDW, respectively. Then, the actual incident laser power density $P = P_0 - P_1 - P_2$. If the radiation loss P_1 in the plasma region is ignored, then $P = P_0 - P_2$. During laser irradiation, the laser acts on the surface of the film to produce a plasma with high temperature and high density. This plasma expands rapidly outward. During the expansion, the plasma continues to absorb the incident laser, so that the laser energy reaching the film will be greatly reduced, preventing the energy coupling between the laser and the film. This effect is called laser plasma shielding. Under the influence of the shielding effect of laser plasma, the laser energy reaching the film surface will gradually decrease, the plasma temperature and density will decrease, the shielding effect of laser plasma will become weak, the plasma absorbs less and less incident laser energy, the laser energy reaching the film will slowly increase, so the plasma temperature and density will rapidly increase, and the plasma shielding effect will be generated. This process is called reverse bremsstrahlung absorption, and the reverse bremsstrahlung absorption coefficient is expressed as [20]:

$$K_s = 9.4675 \times 10^{-42}\lambda^2 {N_e}^2 T^{\frac{3}{2}} Z^2, \tag{10}$$

where N_e represents the electron number density of the film surface material, T represents the plasma temperature, and z represents the atomic number. The actual incident laser power density after considering the reverse bremsstrahlung absorption is P [20], then

$$P = P_0 - P_2 = \frac{P_0}{10^{0.06k_s}}. \tag{11}$$

After the end of the laser pulse, considering the influence of the sparse wave on the LSDW, it is assumed that after the end of the laser pulse, a left-traveling simple wave is reflected on the LSDW, and the time of the first left-traveling simple wave reaching the surface of the film is t_z, which can be expressed as [20]

$$t_z = 2t_p\left(\frac{2\gamma_b}{\gamma_b - 1}\right)^{\frac{\gamma_b+1}{2(\gamma_b-1)}}, \tag{12}$$

where γ_b is the adiabatic index of plasma, and the value in the plasma region is 1.2 [20].

The model used for LSDW motion to study the relaxation process of film surface pressure depends on the three time parameters t_p, t_z, and t_{2D}. There are three cases:

1) When $t_p \le t_z \le t_{2D}$ and $0 \le t_p/t_{2D} \le t_p/t_z$, the axial rarefaction wave reached the film surface before the radial rarefaction wave reached the center of the film surface. When $t_z \le t \le t_{2D}$, the plane attenuation model can be used at that time. When $t \ge t_{2D}$, the cylindrical attenuation model was used. When $t < t_p$, one-dimensional model was used.
2) When $t_p \le t_{2D} \le t_z$ and $t_p/t_z \le t_p/t_{2D} \le 1$, the radial rarefaction wave reached the film surface before the axial rarefaction wave reached the center of the film surface. When $t_p \le t \le t_{2D}$, the plane attenuation model can be used. When $t \ge t_{2D}$, the cylindrical attenuation model was used. When $t < t_p$, one-dimensional model was used.
3) When $t_p \ge t_{2D}$, the radial rarefaction wave reached the film surface before the axial rarefaction wave reached the center of the film surface, and the cylindrical attenuation model was used when $t \ge t_p$.

Assuming $\lambda = 1{,}064$ nm laser-focusing spot diameter $D_s = 0.8$ mm, incident laser energy $E = 0.1$ J, incident laser pulse width $t_p = 10$ ns, and the laser is incident on the surface of a single layer of hafnium oxide film, its t_z equals 2.7×10^{-2} s and t_{2D} equals 5×10^{-8} s. Obviously, $t_p < t_{2D} < t_z$ satisfied the second case. Therefore,

① When $t = 0$, the surface pressure of the film becomes the initial atmospheric pressure $p_0 = 1.013 \times 10^5\,\mathrm{N/m^2}$.

② When $0 < t < t_p$, using one-dimensional model, the pressure p_{s10} of LSDW on the film surface is [20] as follows:

$$p_{s10} = \rho_0 \frac{{v_L}^2}{\gamma_b + 1}\left(\frac{\gamma_b + 1}{2\gamma_b}\right)^{\frac{2\gamma_b}{\gamma_b - 1}}. \tag{13}$$

③ When $t_p \le t \le t_{2D}$, the plane attenuation model can be used, and the pressure of LSDW on the film surface $p_{s2}(t)$ is [20] as follows:

$$p_{s2}(t) = p_{s1}\left(\frac{t_p}{t}\right)^{\frac{2}{3}}. \tag{14}$$

When $t = t_{2D}$,

$$p_{s20} = p_{s10}\left(\frac{t_p}{t_{2D}}\right)^{\frac{2}{3}}. \tag{15}$$

④ When $t \ge t_{2D}$, t_0 is introduced; when $t = t_0$, the surface pressure of LSDW becomes the initial atmospheric pressure p_0, then the plasma flow field has diffused into two dimensions when $t_{2D} \le t \le t_0$, and the cylindrical decay model can be used. The pressure $p_{s3}(t)$ of LSDW on the surface of LSDW is as follows [20]:

$$p_{s3}(t) = p_{s20}\left(\frac{t_{2D}}{t}\right)^{\frac{6}{5}}, \tag{16}$$

By $p_0 = p_{s20}\left(\frac{t_{2D}}{t_0}\right)^{\frac{6}{5}}$,

$$t_0 = t_{2D}\left(\frac{p_{s20}}{p_0}\right)^{\frac{5}{6}}. \tag{17}$$

From Eqs. (13)–(17), the expansion and diffusion of plasma shock wave on the surface pressure $p_s(t)$ of the film is as follows:

$$p_s(t) = \begin{cases} p_0, & t = 0 \\ \rho_0 \dfrac{{v_L}^2}{\gamma_b + 1}\left(\dfrac{\gamma_b + 1}{2\gamma_b}\right)^{\frac{2\gamma_b}{\gamma_b - 1}}, & 0 < t < t_p \\ \rho_0 \dfrac{{v_L}^2}{\gamma_b + 1}\left(\dfrac{\gamma_b + 1}{2\gamma_b}\right)^{\frac{2\gamma_b}{\gamma_b - 1}}\left(\dfrac{t_p}{t}\right)^{\frac{2}{3}}, & t_p \le t \le t_{2D} \\ p_{s20}\left(\dfrac{t_{2D}}{t}\right)^{\frac{6}{5}}, & t_{2D} \le t < t_0 \\ p_0, & t \ge t_0. \end{cases} \tag{18}$$

2.2.2 Impulse per unit area of optical film surface formed by plasma shock wave

Since the area of the optical film is limited, the effective area of the optical film surface for impulse transmission by laser can only be the area of the optical film, and its impulse transmission will be limited by the size of the film area. Assuming that the film area is S and the radius is R, the total impulse transmission time is the total action time t_0 of the laser plasma shock wave. From the previous analysis, it can be seen that $t_p < t_{2D} < t_z$. Therefore, the impulse I_{st} obtained by the film changes from Eq. (5) to the following equation:

$$I_{st} = \int_0^{t_0}\int_S p_s(t)\mathrm{d}S\mathrm{d}t. \tag{19}$$

The following are discussed according to different time intervals:

1) In the range $0 \le t \le t_{2D}$, plasma and shock wave develop in one dimension, and their radial impulse transfer area is approximately the laser spot area $\pi(D_s/2)^2$. During this period, the impulse obtained by the film is as follows:

$$I_{st1} = \pi(D_s/2)^2 \int_0^{t_{2D}} p_s(t)\mathrm{d}t = \pi(D_s/2)^2 \left[3p_{s10}t_p\left(\frac{p_{s10}}{p_{s20}}\right)^{\frac{1}{2}} - 2p_{s10}t_p \right]. \tag{20}$$

2) When $t \ge t_{2D}$, considering the two-dimensional diffusion effect of plasma and shock wave, the lateral

explosion wave is attenuated in the form of the cylindrical explosion wave. According to the cylindrical explosion wave theory, if the time required for the explosion wave to propagate to the film boundary R is t_d, then:

$$R = (D_s/2)\sqrt{\frac{t_d}{t_{2D}}}. \tag{21}$$

Therefore,

$$t_d = t_{2D}\left(\frac{2R}{D_s}\right)^2. \tag{22}$$

Thus, the impulse obtained by the optical film during $t_{2D} \le t \le t_d$ period is as follows:

$$\begin{aligned} I_{st2} &= \pi(D_s/2)^2 \int_{t_{2D}}^{t_d} p_{s20}\left(\frac{t_{2D}}{t}\right)^{\frac{6}{5}}\left(\frac{t}{t_{2D}}\right)dt \\ &= \frac{5}{4}\pi(D_s/2)^2 p_{s20} t_{2D}\left[\left(\frac{t_d}{t_{2D}}\right)^{\frac{4}{5}} - 1\right]. \end{aligned} \tag{23}$$

3) In the range $t_d \le t \le t_0$, the impulse transfer area is limited by the size of the film area, and will not increase any more, but will always be the film area $S = \pi R^2$. During this period, the impulse obtained by the film is as follows:

$$\begin{aligned} I_{st3} &= \pi R^2 \int_{t_d}^{t_0} p_{s20}\left(\frac{t_{2D}}{t}\right)^{6/5} dt \\ &= 5\pi R^2 p_{s20} t_{2D}\left[\left(\frac{t_{2D}}{t_d}\right)^{\frac{1}{5}} - \left(\frac{t_{2D}}{t_0}\right)^{\frac{1}{5}}\right]. \end{aligned} \tag{24}$$

Therefore, the total impulse transmitted to the film during the whole action time is as follows:

$$\begin{aligned} I_{st} = I_{st1} + I_{st2} + I_{st3} &= \pi(D_s/2)^2\left[3p_{s10}t_p\left(\frac{p_{s10}}{p_{s20}}\right)^{1/2} - 2p_{s10}t_p\right] + \frac{5}{4}\pi(D_s/2)^2 p_{s20} t_{2D}\left[\left(\frac{t_d}{t_{2D}}\right)^{4/5} - 1\right] \\ &+ 5\pi R^2 p_{s20} t_{2D}\left[\left(\frac{t_{2D}}{t_d}\right)^{1/5} - \left(\frac{t_{2D}}{t_0}\right)^{1/5}\right]. \end{aligned} \tag{25}$$

2.2.3 Impulse coupling coefficient per unit area of optical film surface formed by plasma shock wave

Impulse energy coupling coefficient can reflect the ability of the film surface to obtain impulse, which is defined as the magnitude of the impulse obtained by the film under the action of unit laser beam energy [20], namely:

$$j = \frac{I_{st}}{E}. \tag{26}$$

The unit of j is N s/J.

When the incident laser wavelength λ = 1,064 nm, the energy E = 0.1 J, the pulse width t_p = 10 ns, the diameter of incident laser beam d = 28 mm, the focal length of the focusing lens f = 350 mm, the distance between the film surface and the focal plane of the focusing lens z_0 = 5 mm, and the film radius R = 5 mm, taking single-layer Al_2O_3 and HfO_2 thin films as examples, the impulse I_{st} and impulse coupling coefficient j of optical thin films per unit area are calculated according to Eqs. (25) and (26). The calculation results are shown in Table 1.

It can be seen from Table 1 that under the same laser action parameters, a single layer of Al_2O_3 thin film with a smaller atomic number Z has a larger impulse and impulse coupling coefficient than HfO_2 thin film, indicating that the single layer of Al_2O_3 thin film has a stronger ability to obtain impulse. In the literature [21], an experimental study on the impulse formation of laser target was carried out. It was found that copper target can obtain more impulse than aluminum target under the same conditions, and the impulse coupling coefficient of copper target and aluminum target is about 10^{-4} N s/J, which is basically consistent with the conclusion in this article. In this article, the impulse coupling coefficient obtained by single-layer aluminum oxide and hafnium oxide film is about 10^{-3} N s/J. The difference in data is mainly caused by the difference in laser parameters and materials.

Different materials have different impulses. The main reason for this phenomenon is that under the action of the same laser action parameters, the effects on plasma and shock waves generated by different films are different. In the process of reverse bremsstrahlung absorption during plasma formation, the reverse bremsstrahlung absorption coefficient is related to the atomic number Z of the film material because the atomic number Z of Al_2O_3 thin film is smaller than that of HfO_2 thin film. As a result, the plasma absorbs more laser energy, expands more violently, and obtains greater impulse.

Table 1: Calculation results

	I_{st} (N s)	j (N s/J)
Al_2O_3 thin film	2.60×10^{-4}	2.60×10^{-3}
HfO_2 thin film	2.27×10^{-4}	2.27×10^{-3}

3 Analysis of factors affecting the impulse of optical film surface formed by shock wave

The variation of I_{st} and j would be studied when the incident laser energy (E), the distance between the film surface and the focal plane of the focusing lens (z_0), the radius of film (R), the focal length of the focusing lens (f), and the incident laser pulse width (t_p) change, respectively.

3.1 Incident laser energy

When the incident laser energy E is changed and other parameters are unchanged (z_0 = 5 mm, f = 350 mm, t_p = 10 ns, R = 5 mm), the curves of I_{st} under different E actions are obtained, as shown in Figure 1. As shown in Figure 1, I_{st} increases with increasing E. And the impulse of the single-layer Al_2O_3 film is larger than that of HfO_2 thin film.

The curve of impulse coupling coefficient j *versus* E is shown in Figure 2. With the increase of E, j decreases, and the impulse coupling coefficient of the single-layer Al_2O_3 thin film is larger than that of HfO_2 thin film, indicating that the ability of the single-layer Al_2O_3 thin film to obtain impulse is stronger than that of HfO_2 thin film.

In 1972, Pirri *et al.* carried out experiments on impulse coupling coefficient of laser-supported detonation wave

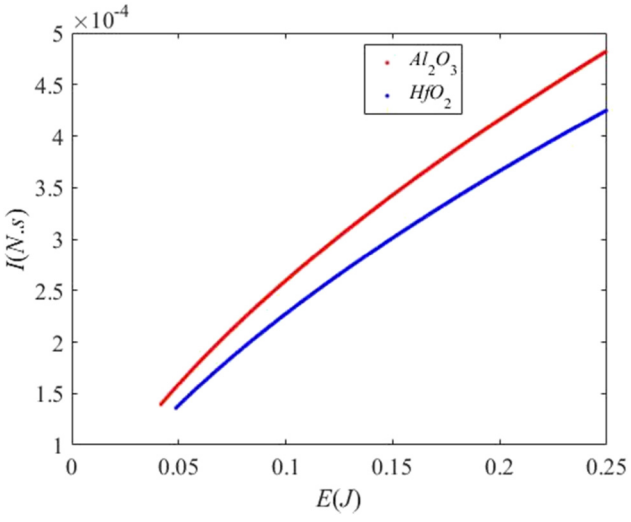

Figure 1: Curves of I_{st} *versus* E (z_0 = 5 mm, f = 350 mm, t_p = 10 ns, R = 5 mm).

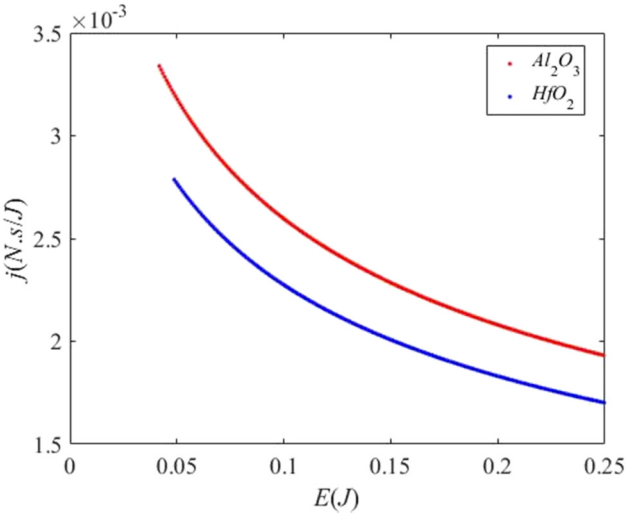

Figure 2: Curves of j *versus* E (z_0 = 5 mm, f = 350 mm, t_p = 10 ns, R = 5 mm).

acting on a flat plate. The experimental results show that the impulse coupling coefficient decreases with the increase of laser incident energy [22]. In 2011, Chen *et al.* also studied the change rule of the impulse coupling coefficient of the plate under the action of laser-supported detonation wave with the laser incident energy, and obtained a conclusion through experiments: the impulse obtained by the plate increases with the increase of the laser incident energy, while the impulse coupling coefficient decreases with the increase of the laser incident energy [23]. The results in these works are basically consistent with the analysis results in this article, but the results given in the works are the change curves of data fitting obtained from experimental measurements, while this study is the theoretical curve obtained from modeling.

3.2 Distance between the film surface and the focal plane of the focusing lens z_0

By changing the distance between the film surface and the focal plane of the focusing lens z_0, other parameters are unchanged (E = 0.1 J, f = 350 mm, t_p =10 ns,R = 5 mm), and the curves of I_{st} *versus* z_0 are obtained, and I_{st} decreases as z_0 increases, as shown in Figure 3. The impulse coupling coefficient j varies with z_0, and j decreases with the increase of z_0, as shown in Figure 4.

In 2007, Zhang *et al.* [24] conducted an experimental study on the influence of defocusing amount z_0 on the mechanical effects of plasma shock waves. The experimental results show that the impulse coupling coefficient

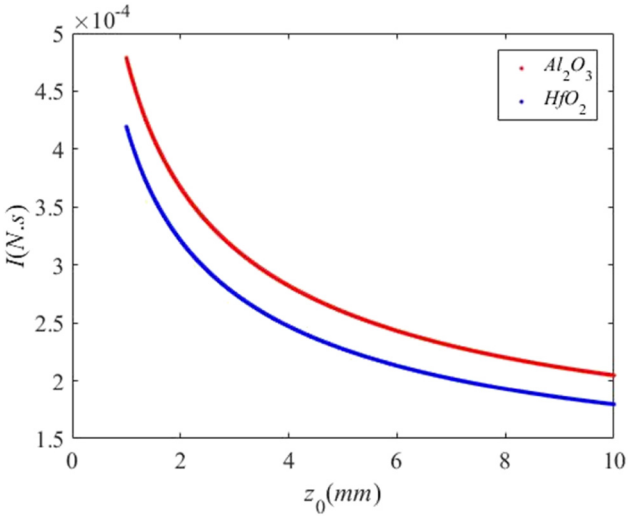

Figure 3: Curves of I_{st} *versus* z_0 (E = 0.1 J, f = 350 mm, t_p = 10 ns, R = 5 mm).

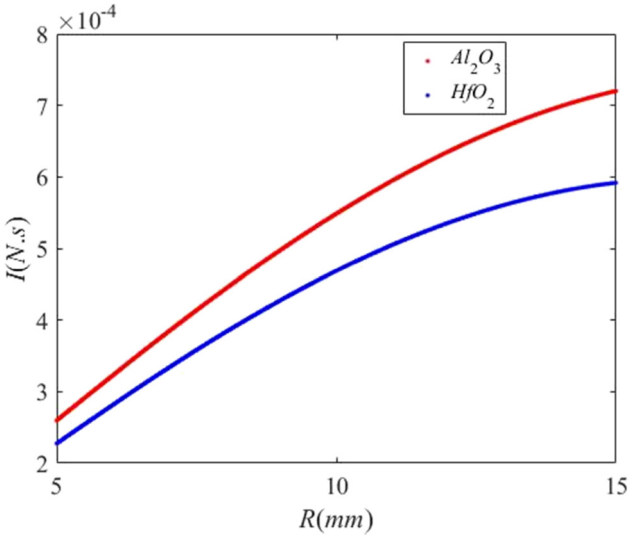

Figure 5: Curves of I_{st} *versus* R (E = 0.1 J, f = 350 mm, t_p = 10 ns, z_0 = 5 mm).

decreases with the increase of z_0, which is consistent with the theoretical analysis results in this study. In 2011, Chen *et al.* [23] obtained the curve of impulse and impulse coupling coefficient changing with defocusing amount z_0, and found that impulse and impulse coupling coefficient decrease with increasing z_0, which is consistent with the conclusion of this study.

This is because as the distance z_0 between the film surface and the focal plane of the focusing lens decreases, the radius of the focusing spot on the film surface will decrease, so the laser power density on the film surface will increase, and the impulse transferred to the film will be greater.

3.3 Radius of film *R*

By changing the radius of film R, other parameters are unchanged (E = 0.1 J, f = 350 mm, t_p = 10 ns, R = 5 mm), and the curves of I_{st} *versus* R are obtained, and I_{st} increases as R increases, as shown in Figure 5. The impulse coupling coefficient j varies with R, and j increases with the increase of R, as shown in Figure 6.

In 2011, Chen *et al.* [23] obtained the curve of impulse and impulse coupling coefficient changing with target area when the critical area of the laser target is 77.33,

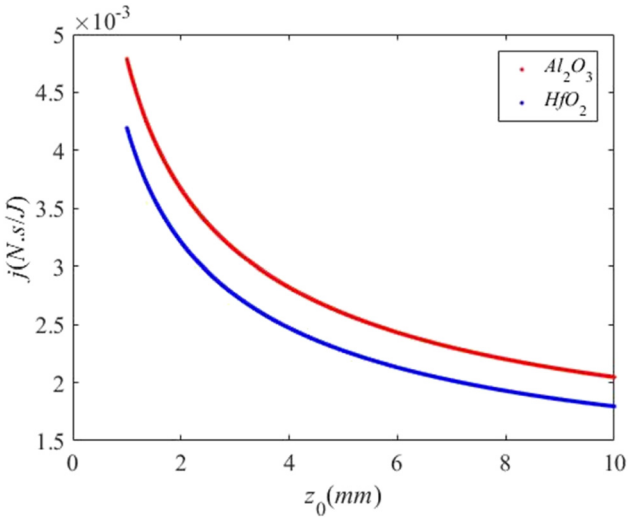

Figure 4: Curves of j *versus* z_0 (E = 0.1 J, f = 350 mm, t_p = 10 ns, R = 5 mm).

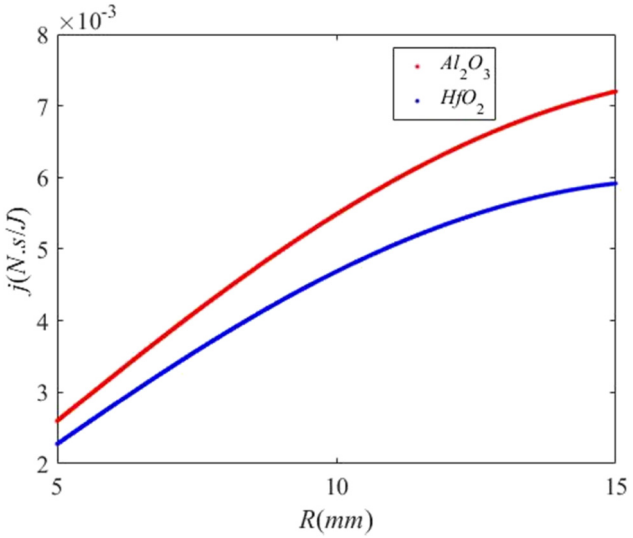

Figure 6: Curves of j *versus* R (E = 0.1 J, f = 350 mm, t_p = 10 ns, z_0 = 5 mm).

113.91, and 128.85 cm^2, respectively. The results showed that impulse and impulse coupling coefficient increase with the increase of target area, and the larger the critical area of the target, the larger the impulse and impulse coupling coefficient. Because the target area is proportional to R, this is consistent with the conclusion in this study.

The size of film radius R has a significant impact on impulse transfer. When the film radius increases, the film area increases, and the impulse transferred to the film also increases, because the impulse transferred to the film is the time accumulation effect of the force, and the action area of the force increases with the expansion of the plasma. Within a certain range, when the film surface area increases, the impulse transferred to the film by the laser also increases, but not unlimited. It can be seen from the previous analysis that the impulse has a total transmission time t_0. When the transmission time is t_0, the corresponding film area is the limit area of impulse transmission. Only the film surface within this limit area has impulse transmission, and there is no impulse transmission beyond this limit area. In addition, when the applied laser energy is small, there is no significant difference in the impulse obtained by the films with different film areas for the same energy. This is because at this time, the limit area of impulse transmission decreases with the weakening of the film surface plasma, so that all the impulses caused by laser plasma can be transmitted to the film.

3.4 Focal length of focusing lens *f*

By changing the focal length of focusing lens f, other parameters are unchanged (E = 0.1 J, z_0 = 5 mm, t_p = 10 ns, R = 5 mm), and the curves of I_{st} *versus* f are obtained, and I_{st} increases as f increases, as shown in Figure 7. The impulse coupling coefficient j varies with f, and j increases with the increase of f, as shown in Figure 8.

Because the focal length f of the focusing lens directly affects the size of the laser focus spot on the film surface, that is, it directly affects the laser power density in the focal spot area, thus affecting the characteristics of plasma generated on the film surface. With the increase of f, the obtained impulse and the impulse coupling coefficient increase.

3.5 Incident laser pulse width t_p

By changing the incident laser pulse width t_p, other parameters are unchanged (E = 0.1 J, z_0 = 5 mm, f = 350 mm, R = 5 mm), and the curves of I_{st} *versus* t_p are obtained, and I_{st} decreases as t_p increases, as shown in Figure 9. The impulse coupling coefficient j varies with t_p, and j decreases with the increase of t_p, as shown in Figure 10.

This is because the larger the t_p is, the smaller the laser power acting on the unit area of the film surface is. Therefore, the smaller the impulse I_{st} and impulse coupling coefficient j formed on the film surface are.

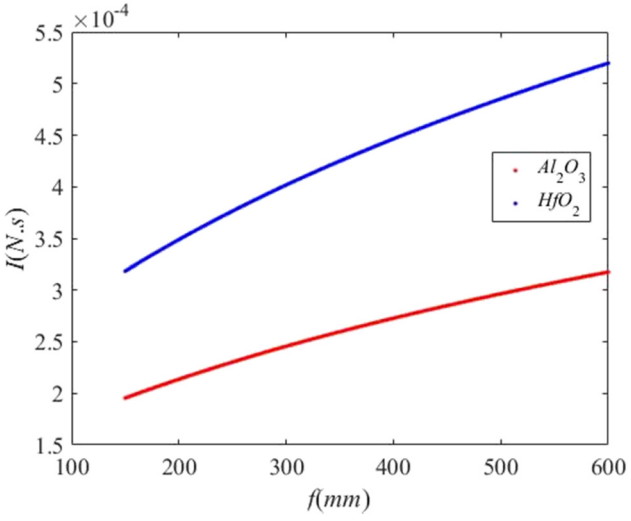

Figure 7: Curves of I_{st} *versus* f (E = 0.1 J, z_0 = 5 mm, t_p = 10 ns, R = 5 mm).

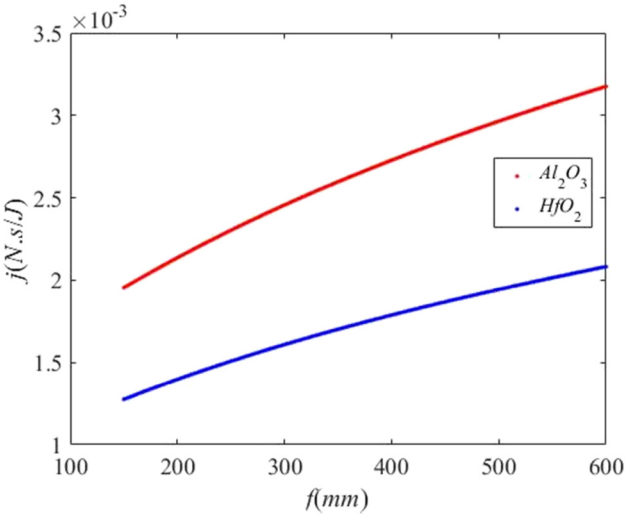

Figure 8: Curves of j *versus* f (E = 0.1 J, z_0 = 5 mm, t_p = 10 ns, R = 5 mm).

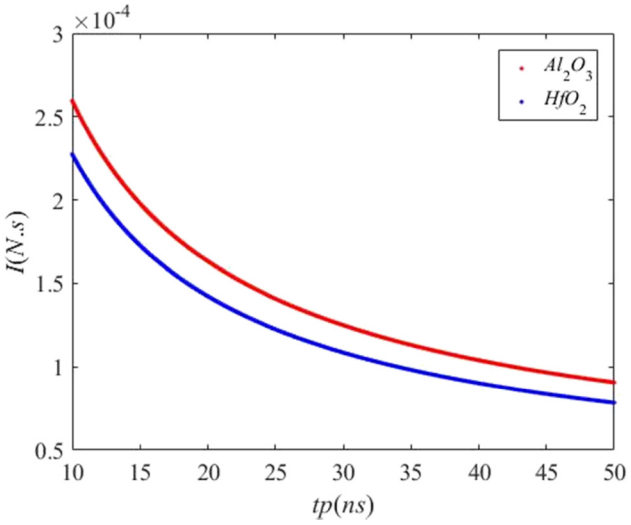

Figure 9: Curves of I_{st} *versus* t_p (E = 0.1 J, z_0 = 5 mm, f = 350 mm, R = 5 mm).

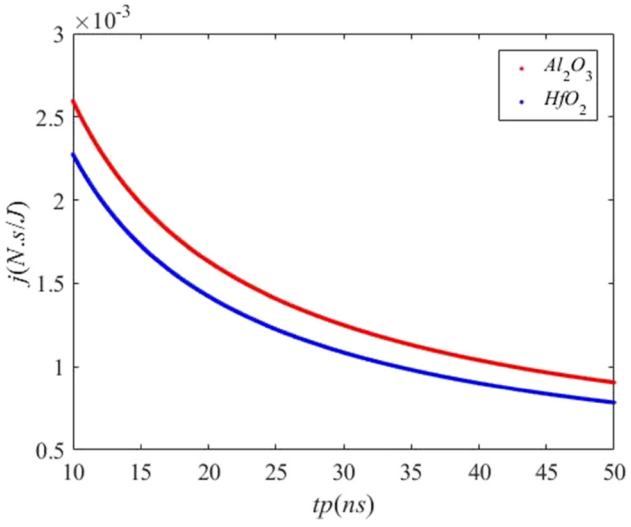

Figure 10: Curves of j *versus* t_p (E = 0.1 J, z_0 = 5 mm, f = 350 mm, R = 5 mm).

4 Conclusion

1) In this study, the impulse calculation model of plasma shock wave acting on the film surface is established. The impulse I_{st} and impulse coefficient j of the single-layer Al_2O_3 and HfO_2 films on the unit area are calculated, respectively, under the specified parameters. The results show that the impulse obtained by Al_2O_3 films is larger, which indicates that I_{st} and j are related to the atomic number Z of the film material. The smaller Z is, the larger I_{st} and j are.
2) The factors affecting the size of I_{st} and j are analyzed. The results show that I_{st} and j of the two films increase with the increase of E and f, and I_{st} and j decrease with the increase of z_0 and t_p. In the total impulse transmission time t_0, I_{st} and j increase with the increase of R, and when the action time exceeds t_0, I_{st} and j are both zero.

The above research shows that the pressure and impulse of the plasma shock wave on the optical film are the factors that cannot be ignored in the process of laser damage to most of the films. Considering that there are also thermal effects, field effects and plasma flash splashing away vaporized film material and other destructive effects in the process of laser damage to the film, it can be asserted that the mechanical effect of plasma shock wave on multilayer optical film, combined with the stress existing in the film, can strengthen the destructive effect of other laser effects on the film system, leading to the collapse of a large area of the film.

In addition, since the laser-supported detonation wave drives the light ship, its propulsion performance is mainly reflected by thrust, impulse, and impulse coupling coefficient. Therefore, the research in this study can also provide theoretical basis for the impulse coupling in laser propulsion technology and the selection of light ship, and has reference significance for the selection of laser parameters, focusing system parameters, and target parameters in laser propulsion research. Since the impulse coupling coefficient is an important parameter to calculate the laser clearance of space debris, this work can also provide a way for the research of laser clearance of space debris.

Funding information: This work was supported in part by the National Natural Science Foundation of China (NSFC) (No. 61378050 and No. 62205263).

Author contributions: All authors have accepted the responsibility for the entire content of this manuscript and approved its submission.

Conflict of interest: The authors state no conflict of interest.

Data availability statement: All data generated or analyzed during this study are included in this published article.

References

[1] Lai QY, Feng GY, Yan J. Damage threshold of substrates for nanoparticles removal using a laser-induced plasma shock-wave. Appl Surf Sci. 2021;539:148282.

[2] Zhu CQ, Dyomin V, Yudin N. Laser induced damage threshold of nonlinear GaSe and GaSe: In crystals upon exposure to pulsed radiation at a wavelength of 2.1 mum. APPL SCI-BASEL. 2021;11(3):1208.
[3] Xie LY, Zhang JL, Zhang ZY. Rectangular multilayer dielectric gratings with broadband high diffraction efficiency and enhanced laser damage resistance. OPT EXPRESS. 2021;29(2):2669–78.
[4] Lian X, Yao WD, Liu WL. KNa2ZrF7:A mixed-metal fluoride exhibits phase matchable second-harmonic-generation effect and high laser induced damage threshold. Inorg Chem. 2021;60(1):19–23.
[5] Shan C, Zhao YA, Zhang XH, Hu GH, Wang YL, Peng XC, et al. Study on laser damage threshold of optical element surface based on Gaussian pulsed laser spatial resolution. Chin J Lasers. 2018;45(1):0104002.
[6] Ling XL, Liu SH, Liu XF. Enhancement of laser-induced damage threshold of optical coatings by ion-beam etching in vacuum environment. Optik. 2020;200:163429.
[7] Kumar S, Shankar A, Kishore N, Mukherjee C, Kamparath R, Thakur S. Laser-induced damage threshold study on TiO2/SiO2 multilayer reflective coatings. Indian J Phys. 2020;94:105–15.
[8] Li YY, Zhang WY, Liu Z, Li MX, Fu XH. Cumulative effect of thin film laser damage under S-on-1 measurement mode. Laser Technol. 2018;42(1):39–42.
[9] Gregg DW, Thomas SJ. Momentum transfer and plasma formation above a surface with a high-power CO2 laser. J Appl Phys. 1966;37(7):2787–9.
[10] Piri AN, Schlier R, Northam D. Momentum transfer and plasma formation above a surface with a high-power CO_2 laser. Appl Phys Lett. 1972;21(3):79–81.
[11] Hettche LR, Tucker TR, Schriempf JT, Stegman RL, Metz SA. Mechanical response and thermal coupling of metallic targets to high-intensity 1.06μm laser radiation. J Appl Phys. 1976;47(4):1415–21.
[12] Duzy C, Woodroffe JA, Hsia JC, Ballantyne A. Interaction of a pulsed XeF laser with an aluminum surface. Appl Phys Lett. 1980;37(6):542–4.
[13] Bass M, Nassar MA, Swimm RT. Impulse coupling to aluminum resulting from Nd: glass laser irradiation induced material removal. J Appl Phys. 1987;61(3):1137–44.
[14] Fu YS, Wang CK. Investigation on the laser-generated stress waves and its application. Laser J. 1984;5(1):1-6,11.
[15] Fu YS, Wang CK. The pressure attenuation of the air spot explode by the laser focusing. Laser J. 1983;4(3):174–5.
[16] Fu YS, Wang CK. Measurement of shock wave pressure induced by intense pulse laser in air - an application of KL-I Sensor. Mech Eng. 1980;2:61–3.
[17] Liang XB, Zhang GP, Fang YW. Research progress of impulse coupling coefficient of pulsed laser to aluminum target fragments. Laser & Infrared. 2020;50(9):1027–34.
[18] Yu CH, Zhou WJ, Chang H, Chen YF. Experimental research on impulse coupling characteristics and plasma plume dynamics of a nanosecond pulsed laser irradiated aluminum target. IEEE Access. 2020;8:205272–81.
[19] Xu YF, Yang L, Zhou DJ, Liu BK, Li QW, Shi WB, et al. Experimental study on the dynamics and parameters of nanosecond laser-induced aluminum plasma. J Phys D Appl Phys. 2022;32(55):325201.
[20] Lu J, Ni XW, He AZ. Physics of interaction between laser and materials. Beijing: China Machine Press; 1996.
[21] Lu J, Ni XW, He AZ. Momentum formation on a target surface with a laser. J Nanjing Univ Sci Technol. 1994;3:61–4.
[22] Pirri AN, Schilier R, Northam. D. Momentum transfer and plasma formation above a surface with a high power CO2 laser. Appl Phys Lett. 1972;21(3):79–81.
[23] Chen L, Lu JY, Wu JY, Feng CG. Laser supported detonation wave. BeiJing: National Defence Industry Press; 2011.
[24] Zhang YZ, Wang GA, Shen ZH, Ni XW, Lu J. Influence of intensity on mechanical effect of laser plasma shock wave. Laser Technol. 2007;(6):659–62.